

## Applications of Intelligent Machine Vision in Plant Factory

Yusuf Hendrawan<sup>\*</sup>, Dimas Firmanda Al Riza<sup>\*</sup>, Haruhiko Murase<sup>\*\*</sup>

<sup>\*</sup>University of Brawijaya, Department of Agriculture Engineering, Faculty of Agricultural Technology, JL. Veteran 65145 Malang, Indonesia (e-mail: yusufhendrawan@gmail.com)

<sup>\*\*</sup>Osaka Prefecture University, Bioproduction Engineering Laboratory, Department of Mechanical Engineering, 1-1 Gakuen-cho Sakai 5998531 Osaka Japan (e-mail: hmurase@me.osakafu-u.ac.jp)

**Abstract:** Intelligent machine vision has been widely used in plant factory for many purposes. There are two aims in this study i.e. the first is improving the performance of intelligent machine vision for precision irrigation system using optimized feature selection technique and the second is developing intelligent machine vision for precision artificial lighting system using Light Emitting Diode (LED). The proposed feature selection technique used in the first aim is Neural-Discrete Hungry Roach Infestation Optimization (N-DHRIO) algorithm. The intelligent machine vision for precision irrigation system and the precision LED lighting system have successfully been developed, and it shows effective to control moisture content and light intensity of the plant precisely. In large scale plant factory, those systems can optimize plant growth and reduce the water consumption and energy costs.

**Keywords:** Plant Factories, Artificial Neural Network, Image Analysis, Pattern Recognition

### 1. INTRODUCTION

A plant factory is defined as a plant production system in under continuous production control throughout the growth period until harvest. A narrow definition is a year-round plant cultivation system in a completely artificial environment (Murase, 2002). There are many commercially operated plant factories, which are heavily equipped with sophisticated environment control systems, machines, instrumentation, and computers. Plant factories can be the best solution for future agriculture (Ioslovich and Gutman, 2000).

Intelligent machine vision has been widely used in plant factory for many purposes. Murase et al. (1997) have implemented intelligent machine vision technique for environmental monitoring in a closed bioproduction system. Bio-response feedback control strategies has been used to develop an intelligent water management system by utilizing intelligent machine vision as non-invasive technique. Intelligent machine vision has also been developed to predict the moisture content of a plant in plant factory. Hendrawan and Murase (2009) used the combination of image features such as: colour, texture, and morphology to predict the moisture content of a plant by using Artificial Neural Network (ANN). Back-propagation Neural Network (BPNN) was used to describe the relationship between moisture content of the plant and image features which were generated from the machine vision. Another applications of intelligent machine vision was precision irrigation system for moss mat production in plant factory as shown in Fig. 1 (Hendrawan and Murase, 2011a; Hendrawan and Murase, 2011b). In those researches, optimization methods such as Neural-Intelligent Water Drops (N-IWD), Neural-Discrete Particle Swarm Optimization (N-DPSO), Neural-Genetic Algorithms (N-GAs), Neural-Simulated Annealing (N-SA), and Neural-Ant Colony Optimization (N-ACO) were used for optimizing the

image feature selection for minimizing the prediction error of moisture content in the plant. When the error to predict the moisture content is low, the irrigation device can give well enough water to the plant as precisely as possible.

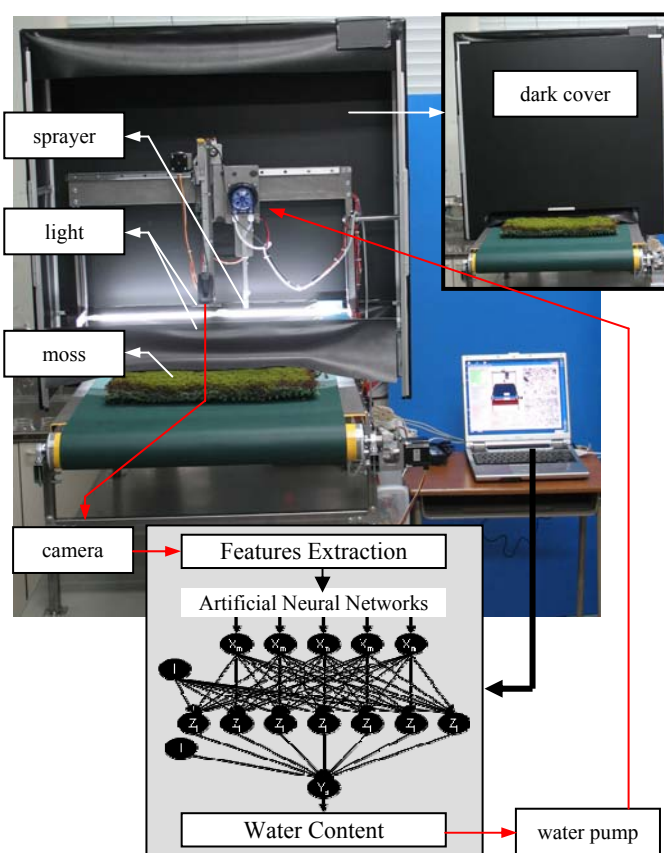


Fig. 1. Intelligent machine vision for precision irrigation system in plant factory.

The recent development of intelligent machine vision is precision artificial lighting system as shown in Fig. 2 (Hendrawan et al., 2012). It is enable us to control the light condition depend on the needs of the plant. The machine vision first identifies how much light is needed in certain areas of the moss mat as precisely as possible, and then to fulfil the light needs as precisely as possible. In the study, a scanning type Laser Diode (LD) was used as light source. LD as light source for plant cultivation has been rapidly developed (Mori et al., 2002). Furthermore, a combination of LD lighting system and machine vision was used to irradiate the specific part of moss mat related to photosynthesis to suppress the energy consumption and optimize the growth of moss in plant factory.



Fig. 2. Precision artificial lighting system for moss mat production using scanning type Laser Diode (LD) lighting system.

There are two aims in this study i.e. the first is improving the performance of intelligent machine vision for precision irrigation system using optimized feature selection technique and the second is developing intelligent machine vision for precision artificial lighting system using Light Emitting Diode (LED). The proposed feature selection technique used in the first aim is Neural-Discrete Hungry Roach Infestation Optimization (N-DHRIO) algorithm.

## 2. MATERIALS AND METHODS

### 2.1 Intelligent Machine Vision for Precision Irrigation

#### 2.1.1 Materials and Equipments

Sunagoke moss mat *Rhacomitrium japonicum* (VARORE Co., Japan) was used in this study. Water content was determined as:

$$\text{Water Content} = \frac{tmw - idw}{idw} \quad (1)$$

where:  $tmw$  is the total moss weight (g) and  $idw$  is initial dry weight (g) of Sunagoke moss. Dry weight of moss was obtained by drying process in the growth chamber (Biotron NK 350, Japan) until there is no decrement in the weight of moss.

#### 2.1.2 Colour Features (CFs)

Colour Features (CFs) include colour mean value and excess RGB index. The equation of colour mean value as follows (Hendrawan and Murase, 2009):

$$\text{colour mean value} = \frac{1}{M} \sum_{i=1}^M \text{colour value} \quad (2)$$

where: colour value can be defined as the range of each colour space in the pixel i.e. red, green, blue, grey, hue, saturation<sub>(HSL)</sub>, saturation<sub>(HSV)</sub>, lightness<sub>(HSL)</sub>, value<sub>(HSV)</sub>,  $X_{(XYZ)}$ ,  $Y_{(XYZ)}$ ,  $Z_{(XYZ)}$ ,  $L^*$ ,  $a^*$ ,  $b^*$ ,  $C_{(LCH)}$ ,  $H_{(LCH)}$ ,  $u_{(Luv)}$  and  $v_{(Luv)}$ .  $M$  is the total number of pixels in the image.

Excess RGB index was calculated by:

$$ER_n = \frac{2R - G - B}{R + G + B}; EG_n = \frac{2G - R - B}{R + G + B}; EB_n = \frac{2B - R - G}{R + G + B} \quad (3)$$

where  $ER_n$ ,  $EG_n$  and  $EB_n$  are the normalized excess Red ( $R$ ) index, excess Green ( $G$ ) index and excess Blue ( $B$ ) index, respectively. The total numbers of CFs are 22 features.

#### 2.1.3 Textural Features (TFs)

One of the most useful parameter in image features is Textural Features (TFs) (Haralick et al., 1973). Some textural features extracted in this study were developed using Colour Co-occurrence Matrix (CCM). The steps to extract TFS are as follows: (1) Transforming RGB colour image to the other colour spaces such as HSL, HSV, XYZ, Lab, LCH, and Luv (Palm, 2004; Leon et al., 2006; Roterman and Porat, 2006; Angulo and Serra, 2007; Kim, 2008); (2) generating CCM from each colour spaces; and (3) extracting TFs using ten Haralick textural equation as follows:

$$\text{Energy} = \sum_i \sum_j P^2[i, j] \quad (4)$$

$$\text{Entropy} = - \sum_i \sum_j P[i, j] \log P[i, j] \quad (5)$$

$$\text{Contrast} = \sum_i \sum_j (i - j)^2 P[i, j] \quad (6)$$

$$\text{Homogeneity} = \sum_i \sum_j \frac{P[i, j]}{1 + |i - j|} \quad (7)$$

$$\text{Inverse Difference Moment} = \sum_i \sum_j \frac{P[i, j]}{|i - j|^k} \quad i \neq j \quad (8)$$

$$\text{Correlation} = \sum_i \sum_j \frac{(i - \mu)(j - \mu)P[i, j]}{\sigma^2} \quad (9)$$

$$\text{Sum Mean} = \frac{1}{2} \sum_i \sum_j (iP[i, j] + jP[i, j]) \quad (10)$$

$$\text{Variance} = \frac{1}{2} \sum_i \sum_j ((i - \mu)^2 P[i, j] + (j - \mu)^2 P[i, j]) \quad (11)$$

$$\text{Cluster Tendency} = \sum_i \sum_j (i + j - 2\mu)^k P[i, j] \quad (12)$$

$$\text{Maximum Probability} = \text{Max}_{i,j} P[i, j] \quad (13)$$

where:  $P(i, j)$  is the  $(i, j)^{\text{th}}$  element of a normalized co-occurrence matrix, and  $\mu$  and  $\sigma$  are the mean and standard

deviation of the pixel element given by the following relationships:

$$P[i, j] = \frac{N(i, j)}{M} \quad (14)$$

$$\mu = \sum_i^M i \sum_j^N P[i, j] \quad (15)$$

$$\sigma = \sum_i^M (i - \mu)^2 \sum_j^N P[i, j] \quad (16)$$

where:  $N(i, j)$  is the number counts in the image with pixel intensity  $i$  followed by pixel intensity  $j$  at one pixel displacement to the left, and  $M$  is the total number of pixels.

The total number of TFs is 190 features. Based on the preliminary research, TFs performed better using the combination of angle ( $\theta = 0$ ) and distance ( $d = 2$ ). Therefore, in this study, TFs were extracted at those values of  $\theta$  and  $d$ .

#### 2.1.4 Back-Propagation Neural Network (BPNN)

A three layers BPNN performed better than the other type of ANN to describe the relationship between moisture content of the moss and the image features. The performance criterion which has been used in this study to test the training, validation, and testing data was Root Mean Squared Error.

$$RMSE = \sqrt{\frac{1}{N_n} \sum_{i=1}^{N_n} (S_i - St_i)^2} \quad (17)$$

where  $N_n$  is number of input (maximum number of input = 112 features),  $S_i$  is the estimated value by BPNN model, and  $St_i$  is the real data of moisture content which can be determined by Eqs. (1). The data which has been used in this study was divided into three components as follows: 325 data as training-set, 162 data as validation-set and 162 data as testing-set.

#### 2.1.5 Multi-Objective Optimization (MOO)

Multi-Objective Optimization (MOO) concerns optimization problems with multiple objectives (Handl et al., 2007). The fitness is calculated as follows:

$$function_1 = weight_1 * RMSE_{(x)} \quad (18)$$

$$function_2 = weight_2 * \frac{IF_{(x)}}{ft} \quad (19)$$

$$fitness(x) = function_1 + function_2 \quad (20)$$

where  $RMSE_{(x)}$  is the validation-set RMSE of ANN using only the expression values of the selected image features in a subset  $x$ , where  $IF_{(x)}$  is the number of image features-subset in  $x$ .  $ft$  is the total image features equal to 112 features,  $weight_1$  and  $weight_2$  are two priority weights corresponding to the importance of the accuracy and the number of selected image features, respectively, where  $weight_1 \in [0.1, 0.9]$  and  $weight_2 = 1 - weight_1$ . In this study, the accuracy is more important than the number of selected image features.

#### 2.1.6 Feature Selection

Selecting features-subset has become the most crucial factor to get optimum result (minimizing the prediction error and

minimizing the number of features-subset). In this study, we introduce the solution to optimize the MOO by using Neural-Discrete Hungry Roach Infestation Optimization (N-DHRIO) algorithm.

There are three simple behaviours of cockroach agents which can be defined as (Havens et al., 2008):

1. *Find\_Darkness*: cockroaches always seek the darkest location. The darkness intensity is directly proportional to the value of the fitness function  $F(x)$ .
2. *Find\_Friends*: cockroaches enjoy being with friends and socialize with the closest cockroaches with the probability per unit time ( $1/\tau_{stop,N}$ ) of stopping when encountering  $N$  friends: 0.49/s for  $N = 1$ , 0.63/s for  $N = 2$  and 0.65/s for  $N = 3$ . If a cockroach comes within a detection radius of another cockroach, then there is a probability of  $1/\tau_{stop,N}$  that these cockroaches will socialize (or group). This socializing phenomenon is imitated in the algorithm as a sharing of information component, where this information is the darkest known location of each individual cockroach which can be defined as personal best solution ( $p$ ). Essentially, when two cockroaches meet, there is a possibility that they will share their knowledge about the darkest location with their neighbours ( $N$ ) and set the darkest local location of the group which can be defined as local best solution ( $l$ ).
3. *Find\_Food*: when a cockroach hungry ( $hunger_i$ ), it will look for food. The food locations are initialized randomly in the search space. The *Find\_Food* behaviour is possibly minimizing the converging to local optima.

The main steps of proposed N-DHRIO for feature selection are as follows:

1. Initialisation of parameters. The maximum iteration ( $t_{max}$ ) is set as the global iteration ( $t_{max} = 500$ ). The number of cockroach ( $N_a$ ) is = 70. For neighbours updating, the parameters are  $A_1 = 0.49$ ,  $A_2 = 0.63$  and  $A_3 = 0.65$ . For hunger updating,  $t_{hunger} = 100$ . The probability of mutation is set  $w = 0.5$ . The probability of crossover is set  $C_o = 0.1; 0.2; 0.3; \text{ and } 0.4$ .
2. Generate roach location ( $x_i$ ) randomly and  $hunger_i = rand\{0, t_{hunger}-1\}$ . Each roach consist of feature-subset (e.g.  $x_i: 1,0,0,0,1,1,0,0,1,1,0,1, \dots, m$ ), where  $m$  is the total features equals to 112 features. Each  $x_i$  in the population expresses a solution to the feature selection problem. A value of 0 indicates that the feature is not selected, while a value of 1 means that the feature is selected.
3. Evaluate each feature-subset ( $x_i$ ) using BPNN.
4. Update the individual solution  $F(x_i)$ . Individual solution  $F(x_i)$  is calculated following the prediction rate (validation-set RMSE) of the evolved subset of features ( $x_i$ ). The input variables of the BPNN are selected image features. One output of BPNN is the moisture content of moss.
5. Calculate neighbours threshold value ( $d_g$ ):

$$M = [M_{jk}] = \frac{\|F(x_j) - F(x_k)\|}{2} \quad (21)$$

$$d_g = median\{M_{jk} \in M : 1 \leq j < k \leq N_a\} \quad (22)$$

6. Repeat steps 6.1 to 6.4 for those  $x_i$  with partial solutions. Steps 6.1 to 6.7 are as follows:
  - 6.1 Updating personal best solution ( $p_i$ ) for the individual cockroach agent:
 
$$p_i \begin{cases} p_i = x_i & \text{if } F(x_i) < F(p_i) \\ p_i & \text{otherwise} \end{cases} \quad (23)$$

- 6.2 Compute the neighbours ( $N_i$ ) of cockroach  $i$ . For  $k = 1$  to  $N_a$ 

$$N_i \begin{cases} N_i = N_i + 1 & \text{if } k : 1 \leq k \leq N_a, k \neq i \text{ AND } M_{ik} < d_g \\ N_i & \text{otherwise} \end{cases} \quad (24)$$

- 6.3 Update the darkest local location or group best solution ( $l_i$ ) according to: For  $r = 1$  to  $N_i$ 

$$l_i \begin{cases} l_i = l_{j_r} = \arg \min_k \{F(p_k)\}, k = \{i, j_r\} & \text{if } \text{rand}[0,1] < A_{\min\{N_i,3\}} \\ l_i & \text{otherwise} \end{cases} \quad (25)$$

where  $\{i, j\}$  are the indices of the two socializing cockroaches and  $p_k$  is the darkest known location for the individual cockroach personal best.

- 6.4 Update roach location ( $x_i$ ):
 
$$x_i \begin{cases} x_i = C_o \oplus CR(C_o \oplus CR(w \oplus MT(x_i), p_i), l_i) & \text{if } \text{hunger}_i < t_{\text{hunger}} \\ x_i = \text{random} & \text{otherwise} \end{cases} \quad (26)$$

The update  $x_i$  consists of three components: The first component is  $a_i = w \oplus MT(x_i)$ , which represents the velocity of the cockroach.  $MT$  represents the mutation operator with the mutation probability of  $w$ . In other words, a uniform random number  $\text{rnd}[0, 1]$  is generated. If  $\text{rnd}[0, 1]$  is less than  $w$  then single insert move mutation operator is applied. The second component is  $b_i = C_o \oplus CR(a_i, p_i)$ , which is the cognition part of the cockroach agent representing the private thinking of the cockroach agent itself.  $CR$  represents the crossover operator between  $a_i$  and  $p_i$  with the probability of  $C_o$ . Two points crossover (point1 and point2) are selected randomly, where  $\text{point1} < \text{point2}$ ,  $\text{point1} > 1$  and  $\text{point2} < m$ . The third component is  $x_i = C_o \oplus CR(b_i, l_i)$ , which is the social part of the cockroach agent representing the collaboration among the group.  $CR$  represents the crossover operator between  $b_i$  and  $l_i$  with the probability of  $C_o$ .

- 6.5 Evaluate each feature-subset ( $x_i$ ) using BPNN.
- 6.6 Update the individual solution  $F(x_i)$  using validation-set RMSE.
- 6.7 Update  $\text{hunger}_i$ :
 
$$\text{hunger}_i = \text{hunger}_i + \text{rand}[0,1] * t_{\text{hunger}} \quad (27)$$
- 6.8 Update iteration-best solution  $T^{TB}$ .
 
$$T^{TB} = \arg \max q(F(x_i)) \quad (28)$$

7. Update the total best solution  $T^{TB}$  by the current iteration-best solution  $T^{TB}$  using:
 
$$T^{TB} \begin{cases} T^{TB} & \text{if } q(T^{TB}) \geq q(T^{IB}) \\ T^{IB} & \text{otherwise} \end{cases} \quad (29)$$

8. Update best feature-subset.

9. Stopping criterion: the algorithm stops with the total-best solution  $T^{TB}$  and best feature-subset. The search will terminate if the global iteration has been reached.

## 2.2 Intelligent Machine Vision for Precision Lighting System

Figure 3 shows the design of intelligent machine vision for precision LED lighting system. The system consists of a set of machine vision which is connected to the image analysis software (built in Visual Basic 6.0), a set of USB controller, and a set of 32 x 32 LED lighting system (combination of Red and Blue LED). First step is image acquisition, and then dividing image into background and object based on the threshold value. ANN was used to determine the intensity level of LED depend on the plant needs. The data is sent using USB controller to the LED panels. The next step is to put the plant under the LED panels and it will provide light intensity to the plant properly. The LED will be OFF if there is no object below it, otherwise it will be ON if there is an object underneath.

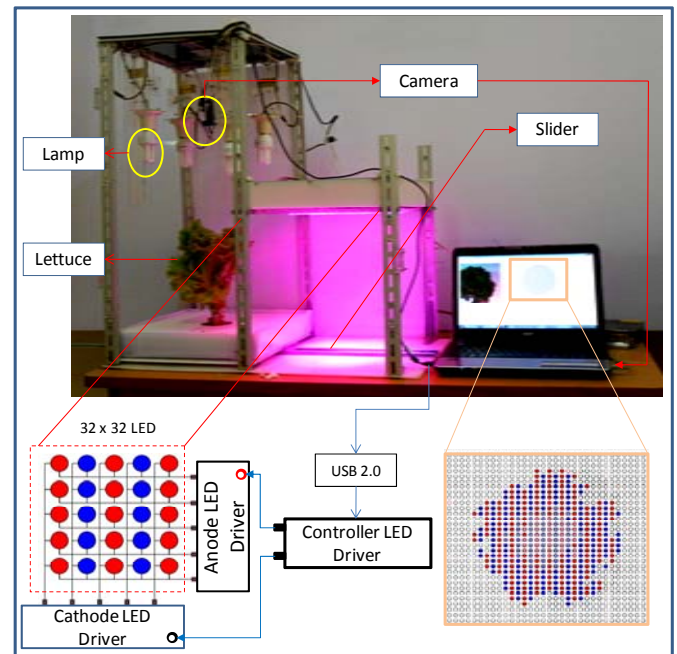


Fig. 3. Design of intelligent machine vision for LED lighting system.

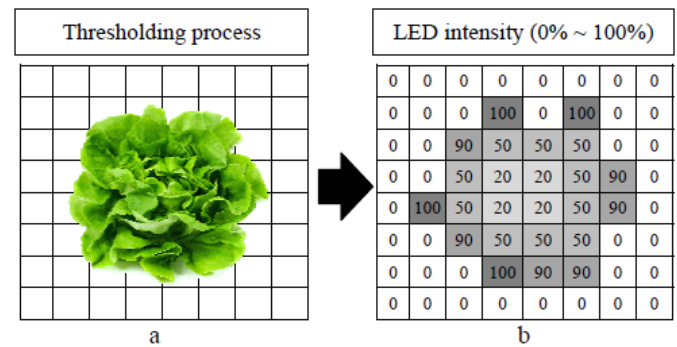


Fig. 4. Image analysis: (a) thresholding process; (b) configuration of LED light intensity.

Figure 4 shows that the object is close to the light source will get a lower light intensity than the object located far from the light source. The ANN's inputs are RGB colour and textural features, while the output is the LED intensity (0% ~ 100%). Lettuce was used as the study samples. Total of 500 samples data were generated for ANN's training-set, validation-set, and testing-set data.

### 3. RESULTS AND DISCUSSION

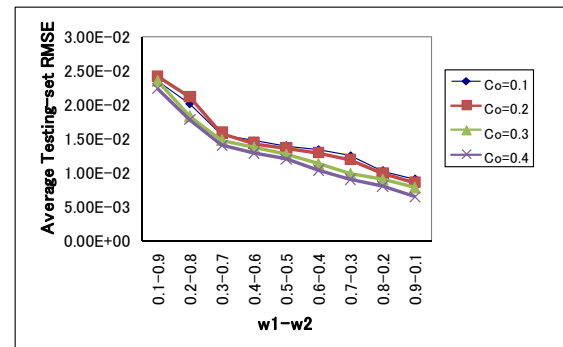
#### 3.1 Performance of Intelligent Machine Vision for Precision Irrigation

Figure 5 shows the performance of N-DHRIO algorithms using different values of  $weight_1$  ( $w1$ ) and  $weight_2$  ( $w2$ ) in 5 runs. The data was trained using various crossover rate ( $C_o = 0.1; 0.2; 0.3; \text{ and } 0.4$ ). Overall, the performance of N-DHRIO as feature selection technique fluctuated because of the diversity of the solutions based on adjusted weights. Moreover, MOO searches simultaneously the solution which is superior in one objective, but poor at others. When the prediction accuracy shows better result, the number of selected image features is larger, and vice versa. The value of  $w1 = 0.1$  and  $w2 = 0.9$  means that the interest rate of the first objective (minimizing the prediction error) is approximately 10%, while the interest rate of the second objective (minimizing the number of features-subset) is approximately 90%. Figure 5(a) shows that the lowest prediction error is at  $w1 = 0.9$  and  $w2 = 0.1$ . In contrast, Fig. 5(b) shows that the smallest number of features-subset is at  $w1 = 0.1$  and  $w2 = 0.9$ . Based on the objective of the MOO, the results show that the best performance of N-DHRIO is using when  $C_o = 0.4$  with the average testing-set RMSE of  $6.37 \times 10^{-3}$  and the average feature subset of 19.3. The plots of best fitness values of MOO using N-DHRIO algorithm are displayed in Fig. 6 to highlight the search process. The best fitness function converged with the lowest testing-set RMSE of  $6.49 \times 10^{-3}$  when using 17 features. From Fig. 6, the fitness value changed and it is getting better until the last iterations (500 iterations). It indicates that feature selection process using N-DHRIO algorithm is effective. Based on this optimum result, we can implement the 17 features which have been selected as the inputs of the ANN to detect the moisture content in the moss. Figure 7 shows the results of BPNN training. The performance results obtained by BPNN in order to make a correlation between the image features as the input and the moisture content as the output is very good. The image features-subset which was used as the input of BPNN was obtained from the result of N-DHRIO as feature selection. The best performance of training-set RMSE of all BPNN models ( $C_o = 0.1$ ; RMSE =  $6.08 \times 10^{-4}$ ); ( $C_o = 0.2$ ; RMSE =  $6.05 \times 10^{-4}$ ); ( $C_o = 0.3$ ; RMSE =  $6.01 \times 10^{-4}$ ); ( $C_o = 0.4$ ; RMSE =  $5.08 \times 10^{-4}$ ) are less than 10%. This shows that the performance of BPNN as learning algorithms is effective (Patterson, 1996).

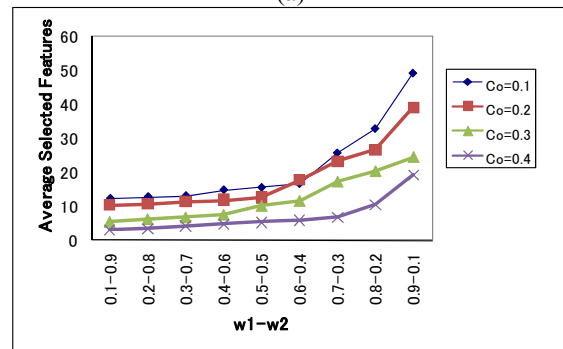
#### 3.2 Performance of Intelligent Machine Vision for Precision Lighting System

Figure 8 shows the performance of BPNN to predict the LED light intensity. It indicates that the performance of BPNN model is satisfactory. The smallest value for training-set

RMSE of the BPNN model is  $6.88 \times 10^{-4}$  and it shows the effectiveness of the learning algorithm. The combination of machine vision and LED lighting system has successfully irradiated the specific areas of the lettuce plant which related to photosynthesis as shown in Fig. 9. It is also applicable to select LED light intensity which is appropriate to the certain part of the lettuce so that all parts of the lettuce can get enough light with proper intensity. In large scale plant factory, this system can reduce the cost of energy.



(a)



(b)

Fig. 5. Performance of N-DHRIO using different values of weights: (a) prediction accuracy; (b) number of selected features.

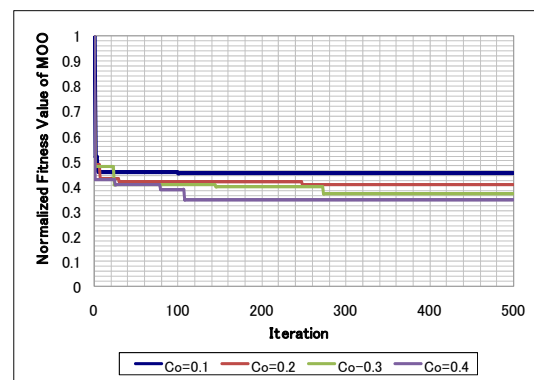


Fig. 6. Plot of best fitness values of MOO.

### 4. CONCLUSIONS

The intelligent machine vision for precision irrigation system using optimized feature selection has been developed. There is an improvement in optimizing feature selection using N-DHRIO compare to the previous study (Hendrawan and Murase, 2011c) using N-GAs, N-ACO, N-SA, N-HBMO, N-IWD, N-FSI. The intelligent machine vision for precision

LED lighting system has also been developed, and it shows effective to select LED light intensity which is appropriate to the certain part of the plant so that all parts of the plant can get enough light and proper intensity. In large scale plant factory, those systems can optimize the plant growth and reduce the water consumption and energy costs.

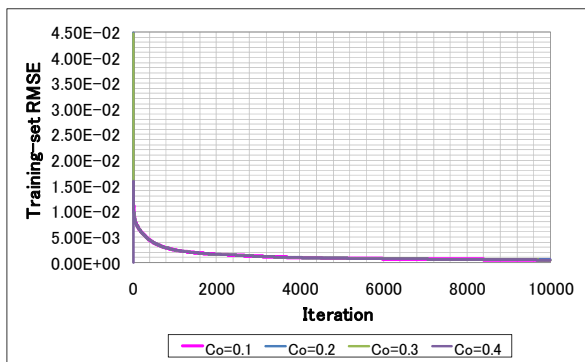


Fig. 7. Learning performance of BPNN using N-DHRIO.

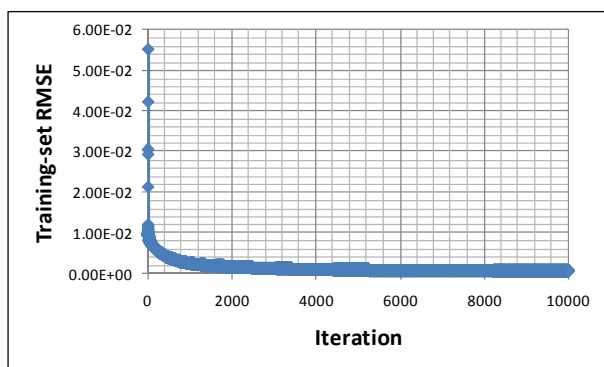


Fig. 8. Learning performance of BPNN for predicting light intensity.



Fig. 9. The result of precision lighting system.

#### REFERENCES

Angulo, J. and Serra, J. (2007). Modelling and segmentation of colour images in polar representations. *Image Vision Comput.* 25, 475-495.  
Handl, J., Douglas, B. K., Knowles, J. (2007). Multiobjective optimization in bioinformatics and computational

biology. *IEEE/ACM T. Comput. BI.* 4(2): April-June 2007.  
Haralick, R. M., Shanmugam, K., Its'hak Dinstein. (1973). Textural features for image classification. *IEEE T. Syst. Man Cyb.* 3(6), 610-621.  
Havens, T. C., Spain, C. J., Salmon, N. G., Keller, M. (2008). Roach Infestation Optimization. *IEEE Swarm Intelligence Symposium.* St. Louis MO USA, September 21-23.  
Hendrawan, Y. and Murase, H. (2009). Precision irrigation for Sunagoke moss production using intelligent image analysis. *Environ. Control Biol.* 47(1): 21-36.  
Hendrawan, Y. and Murase, H. (2011a). Bio-inspired feature selection to select informative image features for determining water content of cultured Sunagoke Moss. *Expert Syst. Appl.* 38: 14321-14335.  
Hendrawan, Y. and Murase, H. (2011b). Neural-Intelligent Water Drops algorithm to select relevant textural features for developing precision irrigation system using machine vision. *Comput. Electron. Agric.* 77: 214-228.  
Hendrawan, Y. and Murase, H. (2011c). Development of Micro Precision Irrigation System in Plant Factory. 18<sup>th</sup> IFAC World Congress, Università Cattolica del Sacro Cuore, Milano Italy, 28 August - 2 Sept., 2011.  
Hendrawan, Y., Argo, B.D., Hermanto, M.B., Zhang S., Murase, H. (2012). Development of a fully controlled plant factory for moss mat production - application of intelligent irrigation system, robot transporter, and precision artificial lighting system. In *The Proceeding of International Conference of Agricultural Engineering CIGR-AGENG 2012.* Valencia, Spain, Valencia Conference Centre, 8 - 12 July, 2012  
Ioslovich, I. and Gutman, P.O. (2000). Optimal control of crop spacing in a plant factory. *Automatica*, 36, 1665-1668.  
Kim, M.C. (2008). Comparative color gamut analysis of xvYCC standard. *Displays.* 29, 376-385.  
Leon, K., Mery, D., Pedreschi, F., Leon, F. (2006). Color measurement in L\*a\*b\* units from RGB digital images. *Food Res. Int.* 39, 1084-1091.  
Mori, Y., Takatsuji, M., Yasuoka, T. (2002). Effects of pulsed-red LD light on the growth of a plant. *Laser Research*, 30(10), 602-605.  
Murase, H. (2002). Precision technologies for protected agriculture. In the proceeding of American Society of Agricultural Engineers (ASAE) Annual International Meeting, Hyatt Regency Chicago, Illinois, USA, July 28 - July 31, 2002.  
Murase, H., Nishiura, Y., Mitani, K. (1997). Environmental control strategies based on plant responses using intelligent machine vision technique. *Comput. Electron. Agric.* 18(2-3): 137-148.  
Palm, C. (2004). Color texture classification by integrative Co-occurrence matrices. *Pattern Recogn.* 37, 965-976.  
Patterson, D.W. (1996). *Artificial neural networks: theory and applications.* Prentice Hall. Singapore.  
Rotterman, Y. and Porat, M. (2006). Colour image coding using regional correlation of primary colours. *Image Vision Comput.* 25, 637-651.